Primary beam shape measurements of the band-2, 125–250 MHz band of the uGMRT

Santaji N. Katore and Dharam V. Lal
snk/dharam AT ncra DOT tifr DOT res DOT in

June 14, 2022

Contents

1 Introduction **3**

2 Old (high-frequency) methodology, data acquisition and data analysis **3**

3 New (revised) methodology and data acquisition **5**
3.1 1-D beam shape 8
3.2 Data analysis 9

4 Systematic trends in the measurements **9**
4.1 Scaling with frequency 9
4.2 Accuracy of fits to the data 10
4.3 Limitations of self-power data 11

5 Summary of Results **11**

6 References **12**

List of Figures

1 The data, the Gaussian fits for three antennas at 150 MHz for the two channels for RR and LL polarisations. 4
2 A 1-D cut along azimuth and elevation axes to the data at 150 MHz. 5
3 Raster scans and the fit to the data at 220 MHz for three antennas for the two channels. . . . 6
4 Raster scans and the fit to the data at 150 MHz for three antennas for the two channels . . . 7
5 Beam width as a function of frequency for three antennas for the azimuth and elevation axes for the RR and LL polarisations. 8
6 Polynomial fits to the beam width at 150 MHz and 220 MHz. 10
7 Beam shape comparisons at 150 MHz and 220 MHz. 11

List of Tables

1 Table listing the coefficients of the 8th order polynomial fit. 9

Abstract

In interferometric images, knowledge of the primary beam is important in measurements of the flux densities and spectra of sources away from the pointing centre. Correction for the effect of the varying primary beam sensitivity is thus important in high dynamic imaging. Here, in this report, we present first measurements of the frequency dependent primary beam shapes for the band-2 (125–250 MHz) of the upgraded GMRT. These measurements would form a useful input for all users of the uGMRT.

1 Introduction

The recently accomplished upgrade of the GMRT (Gupta et al. 2017) has resulted in a significant increase in the instantaneous bandwidth of the telescope. This, it turn, leads to a significant increase in the sensitivity for continuum as well as pulsar studies. As part of the upgrade, all the antenna feeds, except the L-band feed have been replaced. Earlier measurements of the primary beam shape at Band-4 however were available only in the form of the best fit polynomial to an assumed azimuthally symmetric beam. Here we provide measurements of the actual 2-D shape of the beam in each polarisation, which is significantly azimuthally asymmetric, as well as different for the two polarisations. However, for applications in which it is sufficient to assume an azimuthally symmetric polarisation independent beam, we also provide polynomial fits to the same.

Note that the band-2 (125–250 MHz) feeds at the uGMRT are circularly polarised and they have been called as "RR", "LL" and hence, the stokes I is labeled as "RRLL" at the GMRT. In this report, here we continue using this labeling. Here we use these basics (see also 2-D primary beam shape measurements of the band-5, 1050–1450 MHz of uGMRT, S.N. Katore & J.N. Chengalur, and band-4, 550–850 MHz of uGMRT, S.N. Katore & D.V. Lal for more details) and present the methodology in Section 3, data analysis in Section 3.2, and summarize our findings in Section 5.

2 Old (high-frequency) methodology, data acquisition and data analysis

Initially, similar to earlier efforts at band-5 (see S.N. Katore & J.N. Chengalur) and at band-4 (see S.N. Katore & D.V. Lal), here again, the observations were made in the interferometric mode, using observations of 3C calibration sources (3C 286, 3C 48 and 3C 147). We also used the default frequency setup for continuum band-2, 125–250 MHz band observations for all observations.

- Bandwidth = 200 MHz,
- No. of channel = 1024,
- Frequency Range = from 300 MHz to 100 MHz, and
- GAB LO = 300 MHz.

The antennas were scanned in the azimuth axis, with the multiple scans spaced 25′ apart along the elevation axis. The scan rate was 72′/minute and the integration time was either 2 second or 4 second. The grid size was selected to cover the beam at least up to the first null.

After flagging out non functional antennas, the visibilities were used to determine antenna based gains, which was squared to get the power. The known raster scan rate and elevation position were used to convert the time-stamp of the data into the position on in the grid. The solution was computed independently for ∼0.195 MHz wide channels that are spaced ∼5 MHz apart to cover the frequency range from 125 MHz to 250 MHz. The GNUPLOT was used to interpolate the observations onto a uniform grid in altitude and azimuth for each polarisation. A 2-D elliptical Gaussian was fit to each data set using GNUPLOT to parametrize the beam shape.

Unfortunately, this interferometric data have poor SNR (see Figs. 1 and 2), which clearly show departures from symmetric beam shapes or (unrealistic) extent of beam-shapes. We, thus, could not perform the parametrization to study the variation of the beam with frequency and polarisation.

Instead, we next had to resort to the total-power (a.k.a. 'self-power') data to make progress, which we describe below.

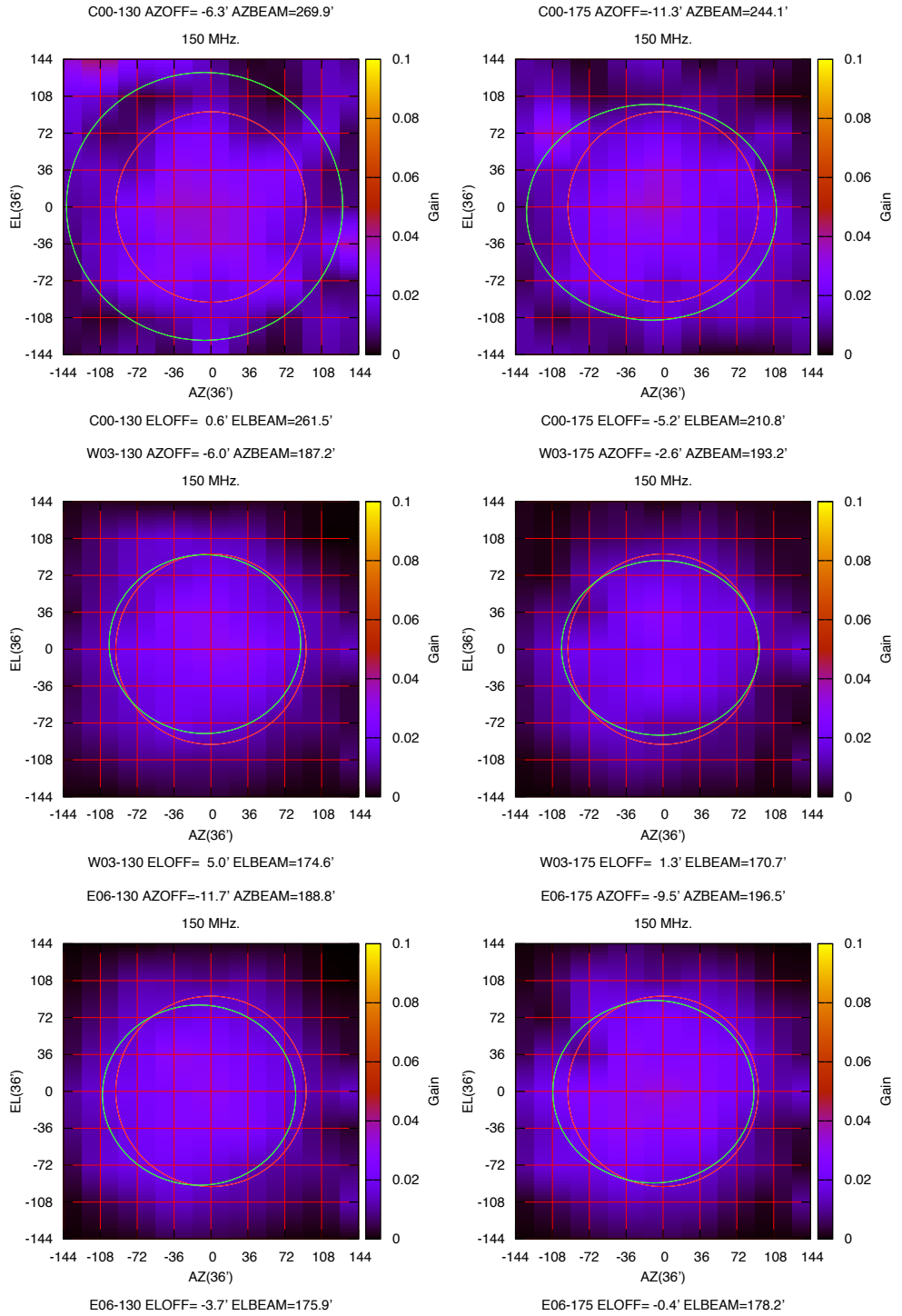

Figure 1: The data, the Gaussian fits for three antennas, C 00, W03 and E06 at 150 MHz for the 130 MHz channel (left-panel) and 175 MHz channel (right-panel) for RR and LL polarisations. The two rings correspond to the expected (red) and observed (blue) polarisations; note the rings are occasionally elliptical showing departures from symmetric beam shape.

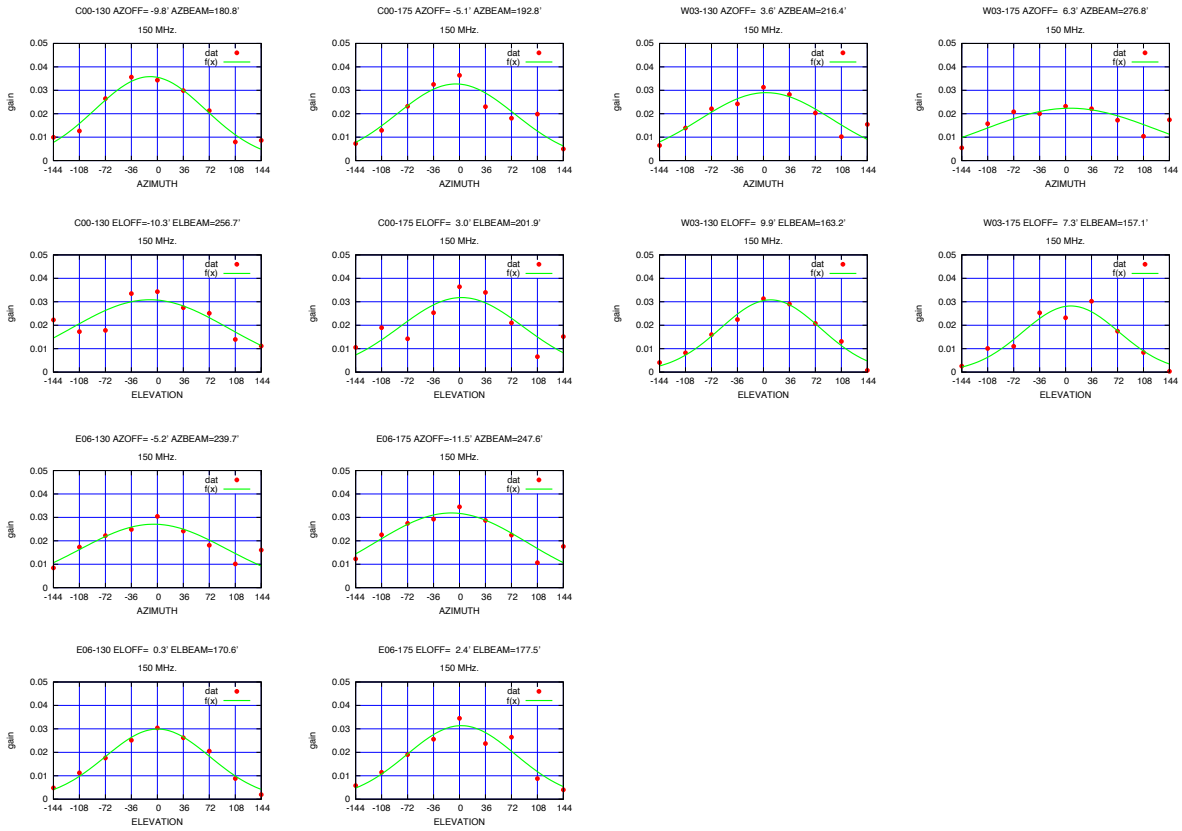

Figure 2: Another realisation of the data presented in Fig. 1 at 150 MHz, a 1-D cut along azimuth and elevation axes. The fit function is used to compute offset and beam-width along the two, azimuth and elevation axes for the two, 130 MHz and 175 MHz channels.

3 New (revised) methodology and data acquisition

Here, in the revised methodology, the observations were thus made in the total-power mode, using observations of strong calibration sources (Cygnus A and Cassiopeia A). We also used the following default frequency setup for continuum band-2, 125–250 MHz band observations for several of our observing runs.

- Bandwidth = 200 MHz,
- No. of channel = 1024,
- Frequency Range = from 300 MHz to 100 MHz, and
- GAB LO = 300 MHz.

The antennas were scanned in the azimuth axis and elevation axis. The scan rate was $67'$/minute and the integration time was either 2 second or 4 second. The scan length was selected to cover the beam at least up to the first null. Note that for high dynamic range imaging applications one would need to determine the primary beam to still further distances than what our measurements provide. One would also need to know the full polarisation properties of the beam. Here, we expect, our measurements should be regarded only as a first step in the direction of characterizing the primary beam.

We performed data analysis only the part of the band where data is present, i.e., between 125 MHz and 250 MHz and below we present our data analysis (Sec. 3.2) and results from parametrization.

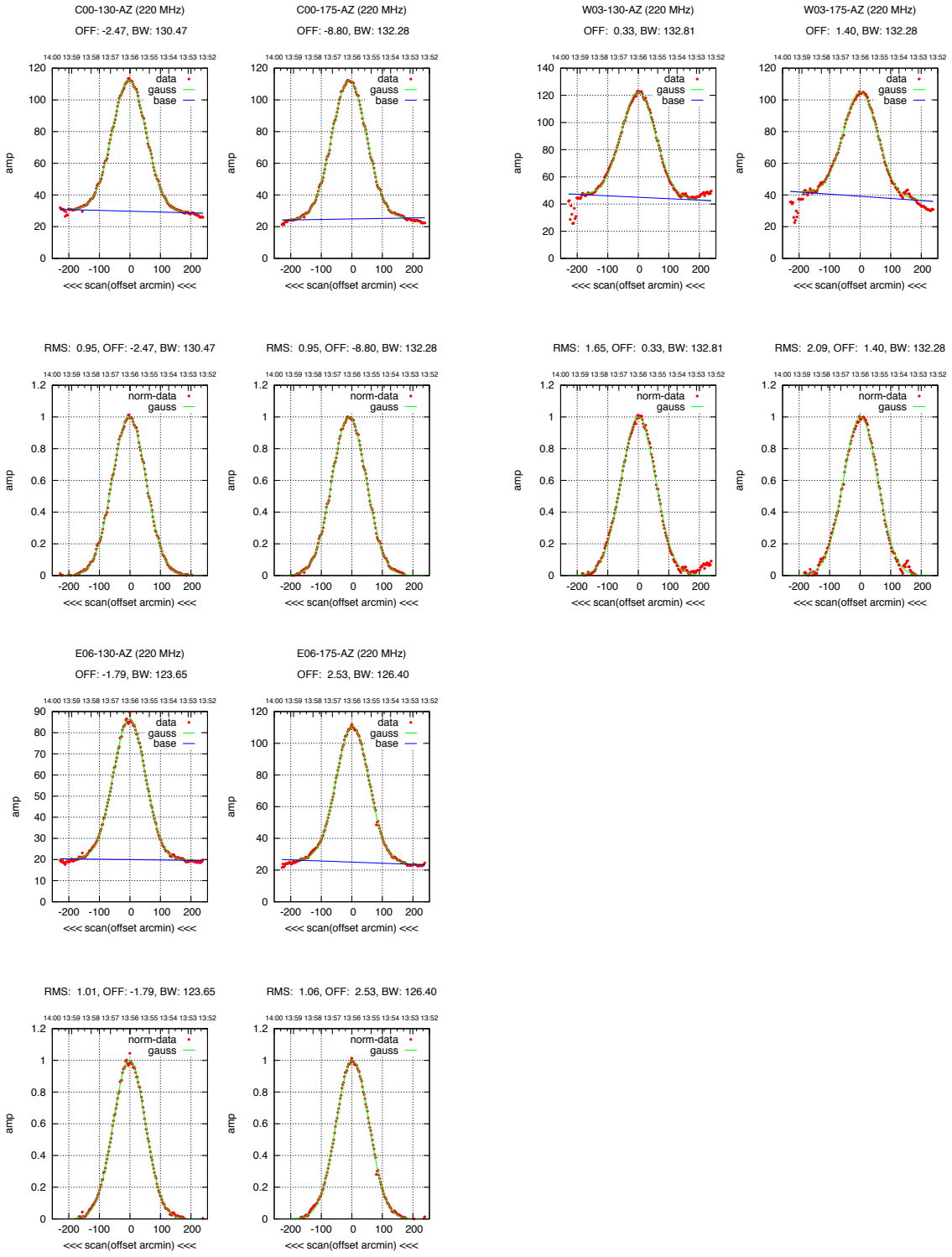

Figure 3: Raster scans of the data at 220 MHz for three antennas, C00 (top-left), W03 (top-right) and E06 (bottom-left). Two columns for each panel shows 130 MHz and 175 MHz channels, where top-row shows the baseline and Gaussian fits fits, and the bottom-row shows fits to the normalised data after setting the peak position to the origin. The fit function comprises of baseline and a Gaussian function is used to correct for the offset and to compute the beam-width along the azimuth axis for the two, 130 MHz and 175 MHz channels.

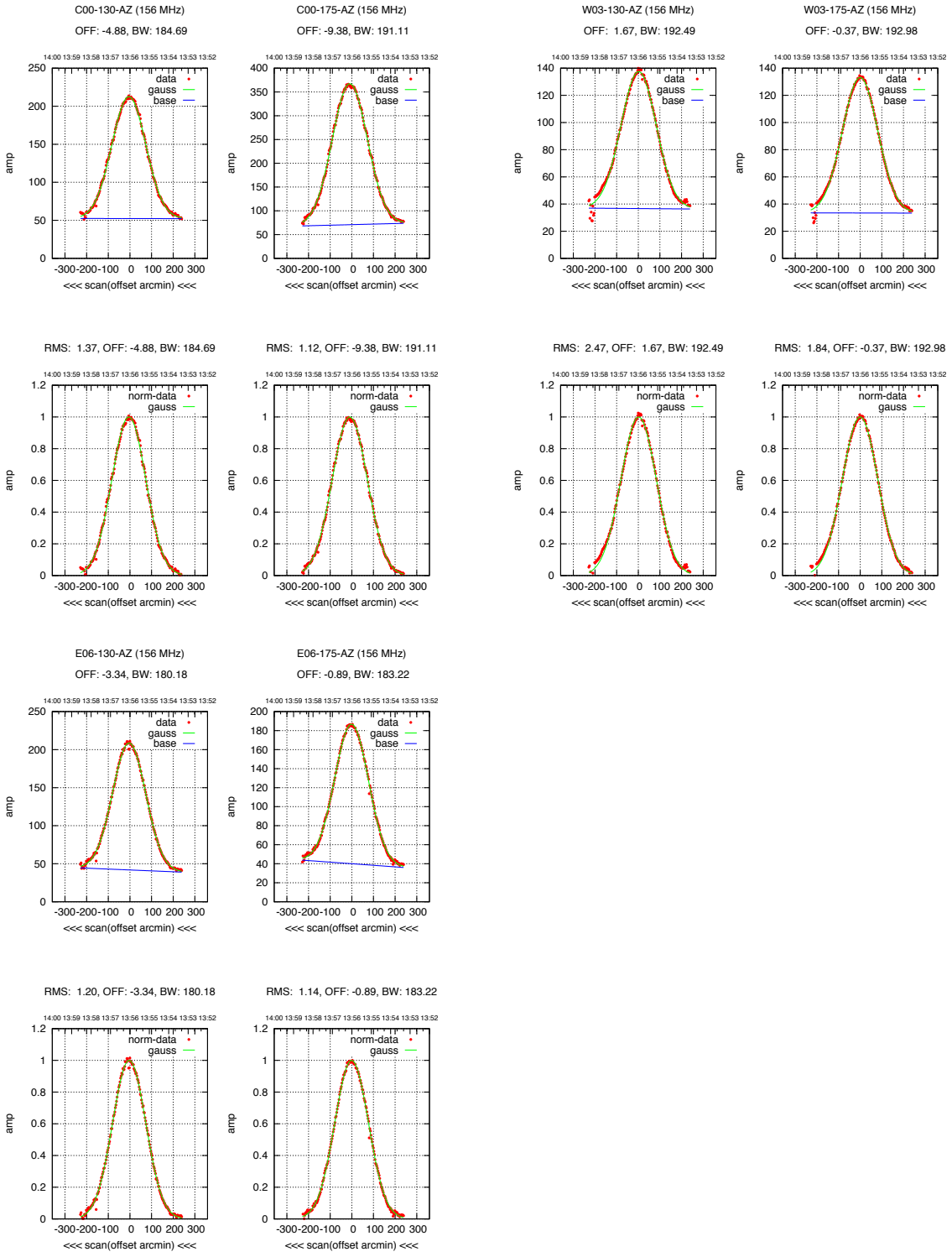

Figure 4: Raster scans of the data at 150 MHz for three antennas, C00 (top-left), W03 (top-right) and E06 (bottom-left). Two columns for each panel shows 130 MHz and 175 MHz channels, where top-row shows the baseline and Gaussian fits fits, and the bottom-row shows fits to the normalised data after setting the peak position to the origin. The fit function comprises of baseline and a Gaussian function is used to correct for the offset and to compute the beam-width along the azimuth axis for the two, 130 MHz and 175 MHz channels.

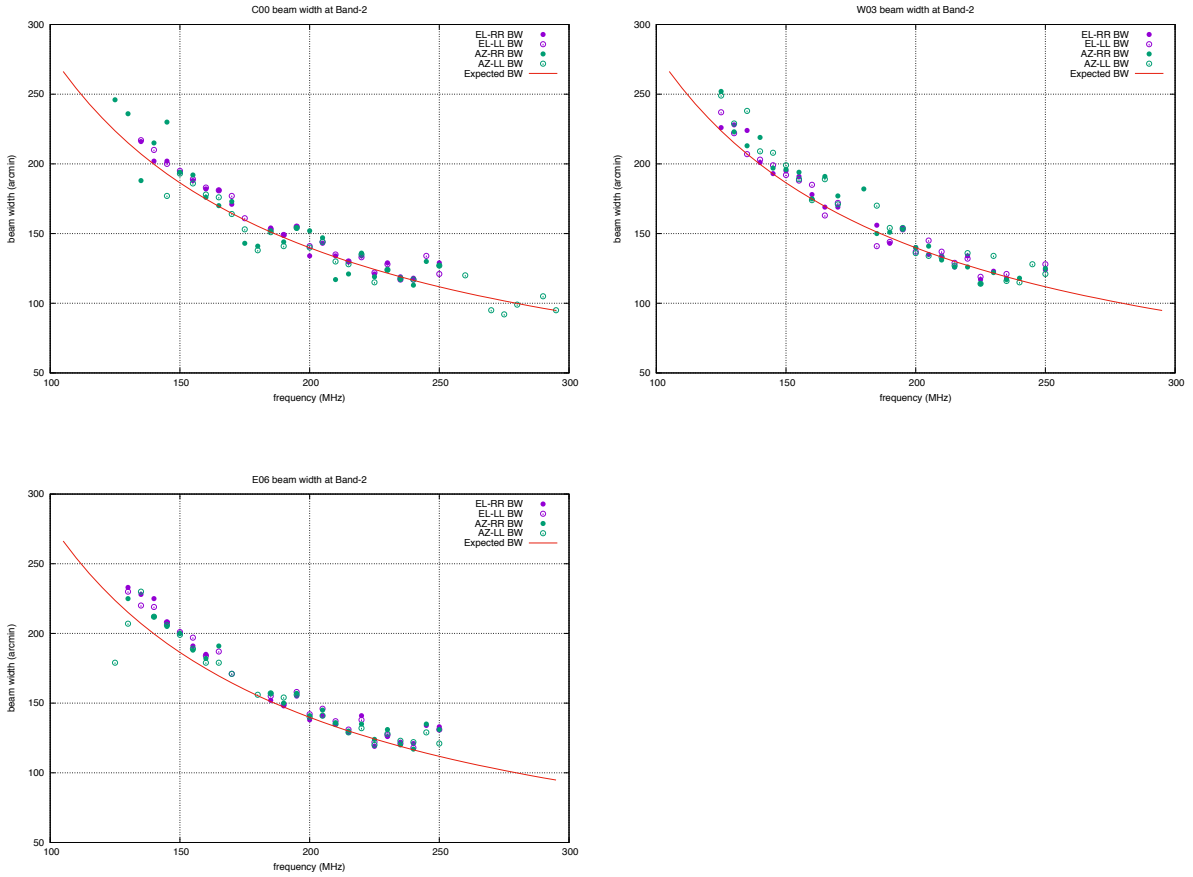

Figure 5: Beam width as a function of frequency for three antennas, C00 (top-left), W03 (top-right) and E06 (bottom-left) for three observing runs dated, 11 February, 15 February and 18 February, respectively. The data for the azimuth and elevation beam widths are plotted in green and magenta, and the RR and LL polarisations are plotted with filled and empty circles, respectively. The smooth red-curve shows (theoretical) expected beam width as a function of frequency.

3.1 1-D beam shape

This parametrization is used to study the variation of the beam with frequency and polarisation. More specifically the 1-D beam data (say, along the azimuth axis) was parametrized using a function of the form:

$$f(x) = A \times e^{-(a(x-x_0)^2)} \tag{1}$$

where,

$$a = \frac{1}{2\sigma_x^2},$$

Here the coefficient A is the amplitude. Note that since we are dealing with the self-power data, we fit a baseline, i.e., a straight line with a slope, which provides a measure of A and the peak position was set to the origin. We thus, together correct for this and perform the Gaussian fit. The x_0 is the offset from the reference center, which here is equal to zero, and σ_x is the spread along x of the beam fit, from which

Table 1: The polynomial coefficients for the 8th order polynomial fit for the raster scan total intensity data. See also Sec. 2 and Sec 3.2.

Order	Polynomial coefficients			
	a	b	c	d
150 MHz	-3.08867	39.31400	-23.01120	5.03731
220 MHz	-3.03366	38.11940	-22.12600	4.81784

the "half power beam width" (HPBW) or "full width at half maximum" can be computed. The HPBW is

$$\mathrm{HPBW} = 2.35482 \times \sigma_x$$

for the x (azimuth) axis. Furthermore, each Gaussian function is normalized to unity at the peak and the peak position was set to (0,0), i.e. the origin (see also Sec. 3.2).

In the similar manner, this data reduction methodology was repeated for the self-power scan along elevation axis. We thus have data along both azimuth and elevation axes for RR and LL polarisations for the two 130 MHz and 175 MHz channels for all (working/good) antennas.

3.2 Data analysis

The methodology discussed above (see Figs. 3 and 4) is used to determine beam-widths at several frequencies, spaced 5 MHz apart across the band for our three observing runs, 11, 15 and 18 February 2022. Note that we performed data analysis for only the part of the band where data is present, i.e., between 125 MHz and 250 MHz and below we present our results from parametrization.

Figs. 3 presents raster scans of the data at 220 MHz for three antennas, C00, W03 and E06. Two columns for each panel shows 130 MHz and 175 MHz channels. We first show the total-power data, together with the baseline and Gaussian fits (see top-row). In the bottom-row, we present the normalised data to unity at the peak, where the peak position was set to the origin, and show the Gaussian fit after removing the baseline fit. Thus, the fit function, which comprises of baseline and a Gaussian function is used to correct for the offset and to compute the beam-width along the azimuth axis for the two, 130 MHz and 175 MHz channels and for the two, RR and LL polarisations.

Similarly, Fig. 4 presents raster scans of the data at 150 MHz for the same three antennas, C00, W03 and E06. Two columns for each panel shows 130 MHz and 175 MHz channels. Here again, we first show the total-power data, and the baseline and Gaussian fits (see top-row). In the bottom-row, we present the normalised data and show the Gaussian fits after removing the baseline fit. Thus, the fit function, which comprises of baseline and a Gaussian function is used to correct for the offset and to compute the beam-width along the azimuth axis for the two, 130 MHz and 175 MHz channels.

In Fig. 5 we present beam width as a function of frequency for three antennas, C00, W03 and E06 for three observing runs. The fit results for azimuth and elevation beam widths and for the RR and LL polarisations show the consistency with the (theoretical) expected beam width (and scatter) as a function of frequency.

4 Systematic trends in the measurements

Below we discuss the dependence of beam-width on the frequency, polynomial fits for an azimuthally symmetric beam profile, and the accuracy of these polynomial fits in order to understand systematic trends, if any in band-2, 125–250 MHz band data of the uGMRT.

4.1 Scaling with frequency

Naively one would expect the beam width to scale linearly with wavelength. However, since the feed illumination may vary in a non trivial manner with wavelength, deviations from this simple scaling are

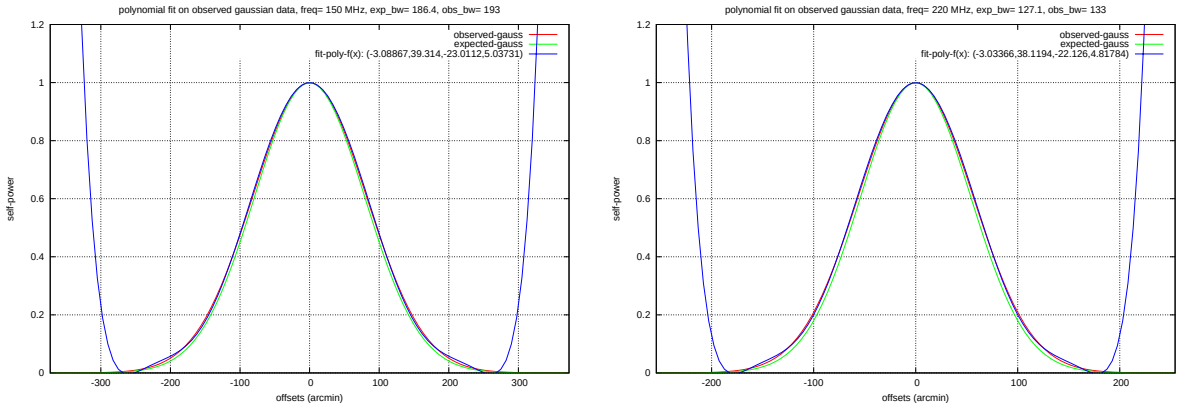

Figure 6: Polynomial fits to the beam width at 150 MHz (left-panel) and at 220 MHz (right-panel). The observed Gaussian and the (theoretical) expected Gaussian are plotted in red and green, respectively. The blue shows the 8th order polynomial fit.

possible. We hence did fits of both first and second order polynomials to the HPBW as a function of frequency, *viz.*,

$$f(x) = \frac{\lambda}{a}$$

is the first order polynomial. Where λ is wavelength, a is the coefficient of the first order polynomial. The Fig. 5 shows the first order polynomial fit to the beam width for three observing runs.

In Fig. 6, we present polynomial fits to the beam width at 150 MHz (left-panel) and at 220 MHz (right-panel). These polynomial fits are derived from the average of the results from the data along both azimuth and elevation axes for RR and LL polarisations for the two 130 MHz and 175 MHz channels of all (working/good) antennas. The observed Gaussian and the (theoretical) expected Gaussian are plotted in red and green, respectively. The blue shows the 8th order polynomial fit to the data in the two panels. The coefficients obtained for the two 8th order polynomials at 150 MHz and at 220 MHz are shown in Table 1. Below we discuss the accuracy of our results, their limitations, etc.

4.2 Accuracy of fits to the data

In order to get an idea as to the expected accuracy of the primary beam correction, ideally the grid-pointing, cross-power data is necessary. In other words the antennas should be scanned in the azimuth axis, with multiple scans spaced appropriately along the elevation axis, and this provides measurements of departures from the symmetric beam-profiles for RR and LL polarisations (see also band-5 and band-4 beam-shape measurements, Katore & Chengalur and Katore & Lal, respectively). Unfortunately, the total power self-data presented here only provides beam-shape measurements along the azimuth and elevation axes and the fit function is the average of these two, and it assumes symmetric profile along 1-D with no offset for the peak position. This reports presently deals only with beam-shape parameters and subsequently, in future, we would be undertaking deep grid-pointing, cross-power measurements.

Nevertheless, we compare beam shape obtained at 150 MHz with the results obtained at 220 MHz and *vice versa*. Fig. 7, left panel shows the (theoretical) expected Gaussian in red and the polynomial using old (legacy) 150 MHz coefficients in green for comparison. Also shown on it are the new uGMRT polynomial at 150 MHz in blue and the new uGMRT polynomial at 220 MHz scaled to 150 MHz in magenta for comparison. Similarly, in the right panel we show these at the 220 MHz, i.e., the (theoretical) expected Gaussian in red and the polynomial using old (legacy) 150 MHz coefficients in green

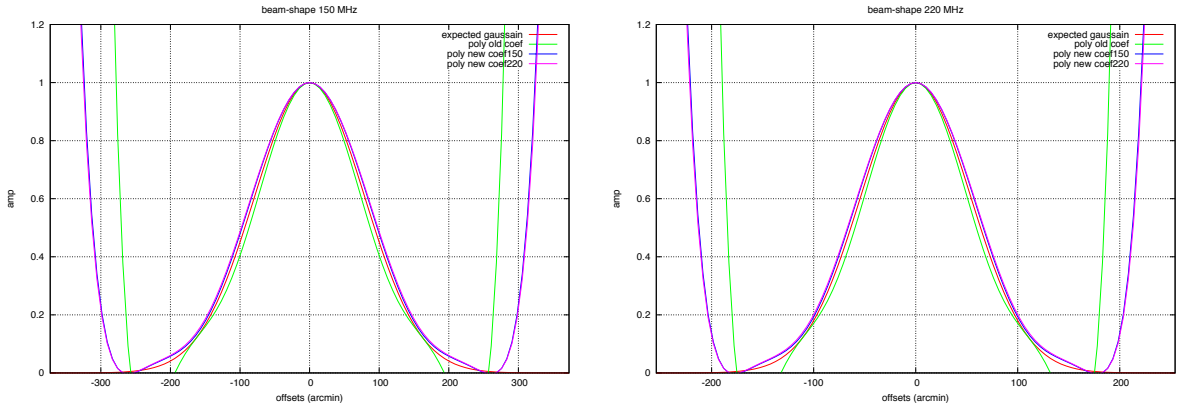

Figure 7: Beam shape at 150 MHz (left-panel): The (theoretical) expected Gaussian is shown in red and the polynomial using old (legacy) 150 MHz coefficients are show in green for comparison. The new uGMRT polynomial corresponding to coefficients shown in Fig.6 (left-panel) are shown in blue. The magenta polynomial corresponds to 220 MHz data that is scaled to 150 MHz frequency for comparison. Beam shape at 220 MHz (right-panel): The (theoretical) expected Gaussian is shown in red and the polynomial using old (legacy) 150 MHz coefficients scaled to 220 MHz frequency are show in green for comparison. The new uGMRT polynomial corresponding to coefficients shown in Fig.6 (right-panel) are shown in blue. The magenta polynomial corresponds to 150 MHz data that is scaled to 220 MHz frequency for comparison.

for comparison; also shown on it are the new uGMRT polynomial at 220 MHz in magenta and the new uGMRT polynomial at 150 MHz scaled to 220 MHz in blue for comparison. This faithful comparison between the beam-shape coefficients at 220 MHz and 150 MHz provides confidence in our methodology.

We note that the polynomial corresponding to old (legacy) 150 MHz coefficients show smaller HPBW at both, 150 MHz and 220 MHz. The reason of this is unclear as we do not have access to the old documentation.

4.3 Limitations of self-power data

Prior to performing baseline correction and Gaussian fit to the data, we need to reference the peak position at the centre of the beam-shape. This essentially removes scope for determining the pointing offset, if any. While, here at the GMRT, we have some form of *a priori* models for pointing offset for each antenna, since we are averaging results from several antennas to determine polynomial coefficients, this information is lost.

The data also does not provide the information on the 2-D shape of the beam-shape, since in the a self-power data is only along azimuth and elevation axes.

We note that our three observing runs, dated 11, 15 and 18 February 2022 did not provide a good baseline at the low end of the frequency, we performed another observing run on 11 March 2022 and went to much larger extent, $\pm$300 arcmin. The fits and the polynomial coefficients from this new data agreed well with the results presented in Fig. 6 and Table 1.

5 Summary of Results

We hope that this document, in particular Table 1 would be useful for the users of the GMRT in order to perform appropriate system checks, thereby improve the performance of the GMRT images at band-2 (125–250 MHz).

In Figs. 6 and 7, we provide comparisons of the beams at the two frequencies 220 MHz and 150 MHz of the 125-250 MHz (band-2) data. They also present the corresponding model beams for the 8th order polynomial fit to the data.

– Clearly there are no appreciable differences that are shown in the data at 150 MHz and at 220 MHz for the 8th order polynomial fit. Henceforth, we will report 8th order polynomial coefficients at 150 MHz.

Although we provide a variety of Figures for users of the uGMRT to make a judgement re. the nature of polynomial fits, we believe that the 8th order polynomial presented here, as was detailed in earlier beam shape documents (e.g., Katore & Chengalur for band-5, Katore & Lal for band-4, and Katore & Lal for band-2, this report) is sufficient to draw science conclusions for the band-2, 125-250 MHz band of the uGMRT.

6 References

– Gupta, Y., et al. 2017 Cu. Sci. 113, 707

– Katore, S. N. & Chengaulr, J. N. 2-D primary beam shape measurements of the band-5, 1050–1450 MHz of the uGMRT

– Katore, S. N. & Lal, D. V. 2-D primary beam shape measurements of the band-4, 550–850 MHz of the uGMRT